An *ab initio* and MNDO-d SCF-MO computational study of stereoelectronic control in extrusion reactions of R_2I–F iodine(III) intermediates†

Michael A. Carroll,[a] Sonsoles Martín-Santamaría,[a] Victor W. Pike,[b] Henry S. Rzepa *[a] and David A. Widdowson[a]

[a] *Department of Chemistry, Imperial College of Science, Technology and Medicine, London, UK SW7 2AY*
[b] *Chemistry and Engineering Group, MRC Cyclotron Unit, Imperial College School of Medicine, Hammersmith Hospital, Ducane Road, London, UK W12 0HS*

Received (in Cambridge, UK) 30th July 1999, Accepted 6th October 1999

MNDO-d and *ab initio* RHF, B3LYP and MP2 energies and geometries are reported for reactant ground and transition states for F–R′ and R–R′ extrusion and R/R′ interconversion reactions of substituted RR′I–F iodine(III) reactive intermediates. The RR′I–F reactant is predicted to form a stable asymmetric bridged dimer involving a square planar iodine centre, hitherto unconsidered as a factor in the chemistry of hypervalent iodine species. Evidence in support of this hypothesis obtained from previously reported crystal structures is discussed. The reactions of both monomer and bridged dimer are found to exhibit unusually large stereoelectronic effects at the iodine centre, deriving from electron donating and withdrawing substituents on the R groups. They are also unusual in showing transition state substituent effects which are opposite to those controlling the ground state stabilities, for which an NBO analysis is presented. Both these effects are manifest in the transition states for reaction of the dimeric species, which is stabilised by electron withdrawing groups present in the pseudo equatorial R′ group of the reacting centre and in the pseudo axial position of the unreacting R component of the dimer.

Introduction

Iodine, like the other halogens, typically exists in a monovalent form (oxidation state −1), but because of its large size and polarisability it is also able to form stable polycoordinate, multivalent compounds. Compounds of this type, containing hypervalent iodine, have been known for over a century and have received considerable interest as both selective reagents and as reactive intermediates.[1] The members of this class of materials that have received the most attention are the diaryliodonium salts, although the use of these species in synthetic chemistry has been somewhat limited, as one of the aryl rings is nearly always phenyl. We have recently overcome this restriction and reported general procedures for the preparation of unsymmetrical and non-phenyl containing diaryliodonium species.[2] Our interest in these materials arose as a result of the demonstration that they are suitable precursors for the formation of fluoroarenes by the capture of fluoride ion by the iodonium salt and subsequent reductive elimination of the iodine(III) intermediate to iodine(I) (Scheme 1).[3]

The ability to control and predict the regiochemical outcome of this aromatic nucleophilic substitution process is of paramount importance. Experimental observations, by us[4] and others,[5] have suggested that these are regiospecific reactions in which specifically the more sterically demanding (the '*ortho* effect') and/or the more electron deficient aromatic ring undergoes preferential nucleophilic substitution. Grushin[5] has proposed that the iodine(III) intermediates in this process are fluxional (Scheme 2) and that the observations can be explained by the 'reactive' R′ group occupying the so-called equatorial position. Whether this property was associated with ground state stability (thermodynamic control) or transition state stability (kinetic control) was not identified.

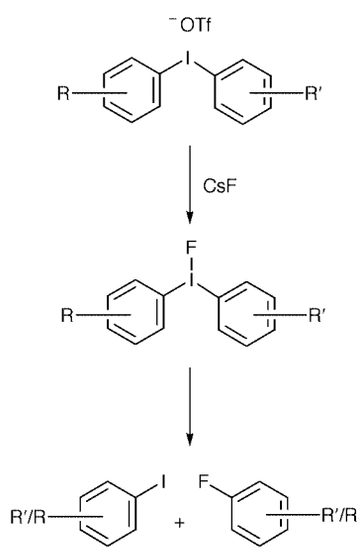

Scheme 1

We have extended this methodology[4] to the introduction of the radioactive ^{18}F label ($t_{0.5}$ = 109.7 min) in the form of $[^{18}F]F^-$. This reagent has distinct advantages over the standard electrophilic procedures, which employ molecular $[^{18}F]F_2$, as it is produced in higher amounts and has higher specific radioactivity by several orders of magnitude.[6] This is an important consideration as ^{18}F labelled organics are employed as radioligands in positron emission tomography (PET), an imaging technique for the absolute measurement, *in vivo*, of positron

† Molecular coordinates in the form of MDL Molfiles, Gaussian or Mopac input files for specific crystal structures and located stationary points are integrated into this article in an enhanced on-line form, together with animations of all important imaginary modes showing the form of the eigenvectors, at the following URL: http//www.rsc.org/suppdata/p2/1999/2707/

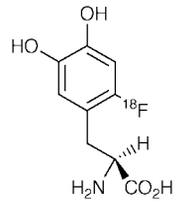

Fig. 1 6-Fluoro-L-DOPA.

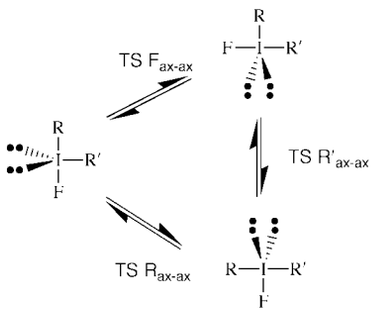

Scheme 2

emitters,[7] enabling their pharmacokinetics and biodistribution to be elucidated by non-invasive means. It is a well established technique as exemplified by the case of 6-[^{18}F]fluoro-L-DOPA[8] (Fig. 1) in the study of brain DOPAmine storage in movement disorders such as Parkinson's disease.

There are several reasons to suggest that the outcome of the nucleophilic substitution process may not be solely dependent on the above factors. The examples in the literature have been restricted to diaryliodonium salts bearing only simple substitution patterns and the previously proposed theories do not adequately explain all of the reported results.[9] Very few computational studies have been carried out for such iodine(III) compounds[10] and we considered that theoretical modelling of these systems might provide an insight into the reactivity of more complicated systems. In the first part of the study reported here, we adopted a strategy of establishing the basic characteristics of the potential energy surfaces at different levels of theory using substituted alkynyl groups as models rather than phenyl groups in order to minimise the computational requirements.

Computational procedure †

Geometries of all species were initially defined using the MacMolPlt program[11] and optimised at the RHF level using the Macintosh implementation of the GAMESS program.[12] All putative saddle points were characterised by calculation of the force constant matrix and normal coordinate analysis, and in selected cases by computing an intrinsic reaction coordinate calculation along the first normal mode direction to verify the identity of the reactants and products deriving from the transition state. The zero point corrections led to a decrease in the activation barriers of between 1.0–1.7 kcal mol^{-1}. Calculations at the B3LYP density functional level were performed using the GAUSSIAN98 program system[13] and at the semi-empirical SCF-MO MNDO-d level using the MOPAC2000 program.[14] Searches of crystal structures were of the Cambridge Structural Database, Version 5.17.[15]

Results and discussion

1. Structures of the reactants RR′I–Z

The ground state geometries for the general system RR′IZ have several points of interest. Crystal structures for both R = alkynyl[16] and R = aryl (in our nomenclature, we reserve X and Y for substituents on the R groups themselves) are known, for which the third iodine ligand Z can be either a halogen (Z = Cl, Br, I), oxygen (Z = OAc, $OCOCF_3$, OTs, OTf, NO_3, ClO_4) or sulfur (Z = xanthate). No X-ray derived structures with Z = F or Z = NR_2 appear to have been previously reported.

Inspection of the geometries[18] of the series Ph_2I–Z (Z = Cl, Br and I) reveals that all three species in fact exist as bridged dimers in which the iodine coordination is best described as square planar, and all eight centres of the dimeric unit are coplanar.[19] For Z = I, the bridge is entirely symmetric, with four equal I···I bonds. For Z = Br, polymorphs exist, one showing only a symmetric bridged dimer, the other indicating the presence of a cyclic tetramer in addition to the dimer. With Z = Cl, there is a small indication of asymmetry in the bridge (I···Cl = 3.105, 3.065 Å). A spacefilling model for this molecule indicates that the van der Waals envelopes of the two iodine atoms slightly inter-penetrate, at an I–I distance of 4.22 Å. No X-ray structure for Z = F has been hitherto been reported.[20] For a symmetric bridge to exist for this system, the I–I distance would have to be approximately 3.7 Å, significantly shorter than the sum of the van der Waals radii. In all cases, the bridge to iodine bond lengths are approximately 0.5 Å longer than those normally found for largely covalent single bonds such as those found for the RIZ_2 series (*e.g.* $PhICl_2$ R_{ICl} = 2.50 Å).[21] Interestingly, symmetric bridged dimers are not found in the RIZ_2 series, although for R = 2,4,6-triisopropylphenyl, Z = Cl, a highly asymmetric weak dimer does occur (R_{ICl} = 2.53, 3.49 Å),[22] the long bridge bond being *anti* to the aryl group and the short one *anti* to the non-bridging Cl group. Other RR′IZ structures (Z = OTs, R_{O-I} 2.56 Å,[23] Z = OTf, R_{O-I} 2.6–2.8 Å,[24] Z = NO_3, R_{O-I} 2.8 Å[25]) show elongated I–O bond lengths compared to $RI(OAc)_2$, R_{I-O} 2.16 Å[26] which appear to indicate some ionic character for the former. The crystal structures indicate that the coordination at the iodine in the RR′I(OR″)$_2$ series is also square planar. Several species involving Z = O coordination reveal further unusual geometries. Thus one species has a I···O bridging (I···O = 2.77 Å) trimeric structure[27] and Ph(PhCC–)I–OTs forms a bridging dimer[16] in which one bridge is a single oxygen (I···O 2.56 Å) and the other a bifurcated O–S–O group from the tosyl moiety.

Two structures in the series RR′BrZ are also known[28] (R, R′ = Ph, Z = Br, I), both forming very similar dimers to the iodine series, again with square planar tetracoordinate bromine atoms. No examples of RR′ClZ where Z = halogen are known, although very recently an example where W = Cl, Z = $SbCl_6$ and R, R′ = -2-adamantylidene has been reported.[29]

Remarkably, the structures of the series RR′W–Z where W is a Group VII element appear to have considerable analogy with those where W is a Group III element. Examples for RR′W–Z, W = B, Al, Ga, In, Tl; Z = F, Cl, Br, I are all known. Where R = mesityl, W = In and Z = F, a symmetric bridged trimer with In–F bond lengths of 2.58 Å is formed.[30] A significant difference from the Group VII series is that the coordination around the indium now approximates tetrahedral, rather than square planar as for iodine. The equivalent Z = Cl structure indicates a symmetric dimer rather than trimer.[31] Increasing the steric hindrance at the *ortho* position of the aryl ring to *tert*-butyl (R = 2,6-di-*tert*-butyl-4-methylphenyl, W = In, Z = Cl)[32] inhibits the bridging halogen entirely. A thallium derivative (R = tetrafluorophenyl, W = Tl, Z = Cl with extra coordination on each Tl from one Ph_3PO) shows a significantly unsymmetric Tl···Cl···Tl bridge (2.54, 2.94),[33] and the most unusual example of this asymmetry is revealed in a R_2B–F system, where a single B···F···B bridging dimer is formed, with B–F bond lengths of 1.43 and 1.65 Å.[34] From the more extensive crystal data reported for the Group III elements, we can draw an inference that asymmetry in the dimeric bridges can be possible, and that using sterically large R groups can inhibit bridge formation.

Having established the (solid state) geometric characteristics of the reagents, we then had to decide how to model the mechanism of reaction of these systems. We firstly noted that the

Table 1 Energies, Hartree (activation barriers, kcal mol^{-1}) and transition normal mode (cm^{-1}) for the stationary point structure X = Y = H

Level of theory	GS F_{ax} (F_{eq})	TS F–R′ extrusion	ν_1	TS F_{ax-ax} interconversion	ν_1	TS R–R′ extrusion	ν_1
1, W = I, Z = F, X = Y = H							
RHF/3-21G(d)	−7138.3465	−7138.2780 (43.0)[a]	634 *i*	−7138.2876 (37.0)[b]	263 *i*	−7138.2550 (57.4)[c]	741 *i*
B3LYP/3-21G(d)	−7142.4747	−7142.4338 (25.7)[d]	456 *i*	−7142.4374 (23.4)[e]	181 *i*	−7142.4196 (34.6)[f]	544 *i*
MP2/3-21G(d)	−7138.3395	−7138.2702 (43.5)	520 *i*				
RHF/DZVP	−7168.9113	−7168.8520 (37.2)	624 *i*	−7168.8668 (27.9)	184 *i*	−7168.8210 (56.7)	758 *i*
B3LYP/DZVP	−7173.0989	−7173.0592 (24.9)	450 *i*	−7173.0681 (19.3)	171 *i*	−7173.0467 (32.7)	552 *i*
RHF/Sadlej pVTZ	−7169.7176	−7169.6517 (41.3)	627 *i*	−7169.6685 (30.8)	192 *i*	−7169.6228 (59.4)	780 *i*
B3LYP/Sadlej pVTZ	−7173.8150	−7173.7698 (28.4)	472 *i*	−7173.7813 (21.1)	171 *i*	−7173.7602 (34.4)	566 *i*
MNDO/d	107.0	166.6 (59.6)	922 *i*	126.2 (19.1)	156 *i*	158.9 (52.07)	822 *i*
2, W = Br, Z = F, X = Y = H							
RHF/3-21G(d)	−2810.6381	−2810.6067 (19.7)	563 *i*	−2810.5875 (31.7)	261 *i*	−2810.5699 (42.8)	732 *i*
B3LYP/3-21G(d)	−2813.8240	−2813.8095 (9.1)	382 *i*	−2813.7940 (18.8)	204 *i*	−2813.7876 (22.9)	533 *i*
RHF/DZVP	−2823.5949	−2823.5662 (18.0)	529 *i*	−2823.5610 (21.2)	169 *i*	−2823.5244 (44.2)	725 *i*
B3LYP/DZVP	−2826.8787	−2826.8606 (11.4)	367 *i*	−2826.8542 (15.4)	178 *i*	−2826.8438 (21.9)	527 *i*
RHF/Sadlej pVTZ	−2824.1726	−2824.1420 (19.2)	540 *i*	−2824.1369 (22.4)	172 *i*	−2824.1010 (44.9)	736 *i*
B3LYP/Sadlej pVTZ	−2827.3714	−2827.3507 (13.0)	385 *i*	−2827.3450 (16.6)	187 *i*	−2827.3351 (22.8)	544 *i*
MNDO-d	136.4	179.4 (42.9)	842 *i*	144.4 (8.0)	27 *i*	173.9 (37.5)	769 *i*
3, Ph_2IF							
RHF/3-21G(d)	−7444.4008	−7444.3341 (41.8)	562 *i*	−7444.3354 (41.0)	212 *i*	−7444.3089 (57.7)	429 *i*
B3LYP/3-21G(d)	−7450.6227	−7450.5769 (28.8)	371 *i*	−7450.5746 (30.2)	131 *i*	−7450.5592 (39.8)	314 *i*
MNSO-d	57.2	110.6 (53.4)	855 *i*	74.0 (16.8)	127 *i*	110.9 (53.7)	690 *i*

[a] Zero point corrected activation energy is 41.5 kcal mol^{-1}. [b] Zero point corrected activation energy is 36.0 kcal mol^{-1}. [c] Zero point corrected activation energy is 55.7 kcal mol^{-1}. [d] Zero point corrected activation energy is 24.3 kcal mol^{-1}. [e] Zero point corrected activation energy is 22.3 kcal mol^{-1}. [f] Zero point corrected activation energy is 33.0 kcal mol^{-1}.

dimer formation noted above has not hitherto been considered as an important factor in previous studies of these systems. Before considering this factor in the mechanism, we felt it imperative to characterise the gas phase potential energy surfaces for the pure monomeric RR′I–Z species, and then to study the perturbation on this surface resulting from dimer formation. The next objective was to establish reliable computational procedures for the reaction potential surfaces for the model systems shown in Scheme 3. We decided to use the semi-

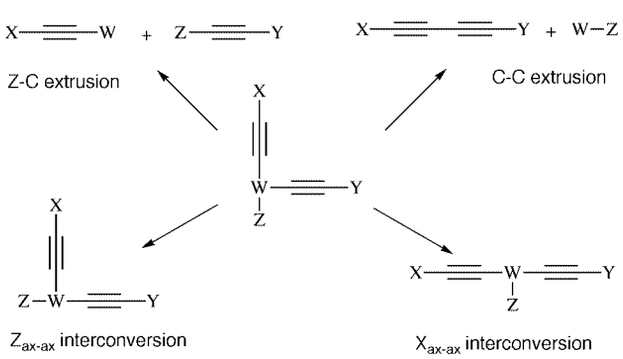

Scheme 3

empirical MOPAC method using the MNDO-d parameter set, which includes d-functions on iodine, as a rapid prototyping method. This would be followed by calculations at the *ab initio* level using basis sets such as 3-21G(d), a DZVP double zeta basis optimised for density functional calculations[35] and the Sadlej[36] pVTZ triple zeta basis set which includes f functions to establish more reliable energetics. The *ab initio* calculations would be performed at the Hartree–Fock (HF), the B3LYP density functional and the MP2 correlated levels.

2. The prototypic unsubstituted systems. Reaction pathways for monomeric reactants

For the prototypic system where R = alkynyl (X = Y = H), W = I and Z = F the energies at these levels (Scheme 3), of the two ground states (Z = axial and Z = equatorial) and four transition states (F–R′ extrusion, R–R′ extrusion, and fluxional interconversion *via* Z_{ax-ax} or *via* R_{ax-ax}) were calculated (Table 1). All the theoretical methodologies predict that the fluorine substituent (Z = F) is significantly more stable in the axial compared to the equatorial position (18.2, 13.7 and 16.0 kcal mol^{-1} at RHF/3-21G(d), B3LYP/3-21G(d) and MNDO-d level respectively). Interconversion of the R and R′ groups (*i.e.* CC–X with CC–Y in Scheme 3) in the monomer is predicted to proceed directly *via* a Z_{ax-ax} transition state rather than to involve an alternative pathway involving a Z_{eq} intermediate (Scheme 2) which is calculated to be significantly higher in energy. The calculated energies of both extrusion reactions are higher than R/R′ interconversion, suggesting that for this system, the fluxional behaviour represents a pre-equilibrium to the rate determining extrusion steps. These results are not significantly changed by improving the quality of the 3-21G(d) basis set to a full double zeta +polarisation and to a triple zeta level. In particular the relative energies of the two extrusion transition states are still higher than the fluxional transition state by at least 5 kcal mol^{-1}. We note below that an alternative mechanism for fluxional behaviour in fact decreases this barrier further. These results suggest that use of the 3-21G(d) basis set is adequate for relative comparisons of substituent effects.

The barriers to reaction at the Hartree–Fock level are significantly higher than those expected for a thermally facile reaction, whilst the correlated B3LYP and MP2 values are more reasonable for such a reaction.[37] The MNDO-d results show some significant variations from the *ab initio* results. In particular, the barrier for C–C extrusion is lower than for F–C extrusion, the barrier for R/R′ interconversion is significantly smaller whilst that for F–C extrusion significantly higher than the B3LYP/3-21G(d), B3LYP/DZVP or B3LYP/Sadlej pVTZ results. Finally in this calibration we included B3LYP/3-21G(d) results for **3**, R = Ph instead of the smaller R = alkynyl system. The results were very similar, the only significant difference being that now the B3LYP/3-21G(d) barrier for R/R′ interconversion was only 1–2 kcal mol^{-1} lower than the extrusion reaction. As suggested below, a mechanism for R/R′ interconversion involving dimers provides a much lower energy

Table 2 Energies (activation barriers, kcal mol^{-1}) and transition wavenumber (cm^{-1}) for stationary point structures (RHF/3-21G(d)/Hartree, **B3LYP/3-21G(d)/Hartree**, *MNDO/kcal mol*$^{-1}$)

Entry	TS F–R′ extrusion	ν_1	TS F_{ax-ax} interconversion	ν_1	TS R–R′ extrusion	ν_1
4,[a] W = I, Z = F, X = CN, Y = H	−7229.4933 (46.5)	663 *i*	−7229.5042 (40.8)	262 *i*	−7229.4755 (57.7)	729 *i*
	−7234.1711 (28.9)	**473** *i*	**−7234.1751 (25.4)**	**183** *i*	**−7234.1625 (34.4)**	**533** *i*
	195.5 (62.3)	*945 i*	*145.6 (12.4)*	*37 i*	*184.2 (51.0)*	*786 i*
5,[a] W = I, Z = F, X = H, Y = CN	−7229.5057 (35.0)	553 *i*	−7229.5042 (36.0)	262 *i*	−7229.4770 (53.0)	725 *i*
	−7234.1796 (20.4)	**398** *i*	**−7234.1751 (22.6)**	**183** *i*	**−7234.1624 (31.5)**	**520** *i*
	186.8 (50.9)	*835 i*	*145.6 (9.7)*	*37 i*	*182.2 (46.3)*	*762 i*
6,[b] W = I, Z = F, X = OCH_3, Y = H	−7251.5289 (41.1)	610 *i*	−7251.5371 (36.0)	260 *i*	−7251.5050 (56.1)	768 *i*
	−7256.3285 (24.4)	**433** *i*	**−7256.3304 (22.5)**	**188** *i*	**−7256.3139 (33.9)**	**527** *i*
	125.3 (59.4)	*910 i*	*85.7 (19.8)*	*161 i*	*116.0 (50.1)*	*781 i*
7,[b] W = I, Z = F, X = H, Y = OCH_3	−7251.5186 (48.2)	652 *i*	−7251.5371 (36.6)	260 *i*	−7251.5007 (59.4)	731 *i*
	−7256.3203 (30.6)	**459** *i*	**−7256.3304 (23.3)**	**188** *i*	**−7256.3092 (37.7)**	**557** *i*
	122.3 (55.4)	*862 i*	*85.7 (18.8)*	*161 i*	*116.5 (49.7)*	*772 i*
8,[c] W = I, Z = F, X = CN, Y = OCH_3	−7342.7350 (52.7)	682 *i*	−7342.7551 (40.1)	260 *i*	−7342.7229 (60.3)	722 *i*
	−7348.0589 (32.3)	**481** *i*	**−7348.0700 (25.3)**	**199** *i*	**−7348.0545 (36.2)**	**544** *i*
	151.6 (59.6)	*877 i*	*113.1 (20.3)*	*162 i*	*141.7 (48.9)*	*735 i*
9,[c] W = I, Z = F, X = OCH_3, Y = CN	−7342.7588 (32.6)	531 *i*	−7342.7551 (35.0)	259 *i*	−7342.7320 (49.4)	719 *i*
	−7348.0770 (17.3)	**371** *i*	**−7348.0700 (21.7)**	**199** *i*	**−7348.0617 (27.7)**	**497** *i*
	145.0 (50.3)	*822 i*	*113.1 (18.4)*	*162 i*	*138.1 (43.4)*	*698 i*

[a] Relative ground state energy **5**–**4**; −3.70, **−2.86**, *−2.71* kcal mol^{-1}; Relative transition state energy **5**–**4**; +7.78, **+5.33**, *+8.72* kcal mol^{-1}. [b] Relative ground state energy **7**–**6**; +0.63, **+0.76**, *−1.02* kcal mol^{-1}; Relative transition state energy **7**–**6**; −6.46, **−5.15**, *+2.96* kcal mol^{-1}. [c] Relative ground state energy **9**–**8**, −5.15, **−3.65**, *−2.71* kcal mol^{-1}; Relative transition state energy **9**–**8**, +14.93, **+11.36**, *+6.66* kcal mol^{-1}.

pathway for this process, and hence we feel fairly confident that these reactions are likely to be kinetically controlled by the stability of the transition state, rather than thermodynamically controlled by the energies of the ground state reactants.

3. Reaction pathways for monomeric substituted systems

Having established that the small 3-21G(d) basis set gives results consistent with larger basis sets, we next proceeded to investigate various combinations of the substituents X and Y on the prototypic reaction with Z = F, and W = I. The reagents (Tables 2 and 3) were invariably predicted to be more stable in the cases where the alkynyl groups bearing electron-withdrawing substituents were placed in the axial position (entries **4**, **8** and **12**) and the electron-donating substituents in the equatorial position (entries **7**, **8**, **11** and **12**). This is inconsistent with the experimental observation that F_{ax}–R_{eq} insertion occurs onto the substituent bearing the electron-withdrawing group.

The transition state energies however revealed different behaviour. These indicate very clearly that the less stable reagents generate the *more* stable transition states for F–C insertion, which is indeed consistent with experiment, and which tends to suggest that our assumed model of a predominantly covalent I–F bond is not unreasonable. Thus the calculations clearly suggest that reaction proceeds by attack on the most electron-deficient alkynyl group placed on the equatorial position (*e.g.* entries **5**, **6** and **9**). The computed barriers for the axial–equatorial interconversion of the fluorine for entries **4**, **6**–**8** were less than for the F–R′ extrusion. Such a pre-equilibrium interconverting the reactants (*e.g.* **6** and **7**) would mean that the regioselectivity of the reaction would be determined purely by the relative energies of the two transition states, and not by the stability of the reactant. Only in the cases where the cyano substituent was placed in the equatorial position (**5** and **9**, Table 2) were the (monomeric) fluxional barriers predicted to be bigger than for the F–C extrusion. We address this aspect further in our discussion below on the dimeric reagents. This substituent effect arises because the "push-pull" substituent combination (**9**, X = OMe, Y = CN) in particular decreases the barrier to extrusion compared to X = Y = H by 15 kcal mol^{-1} at the B3LYP/3-21G(d) level, whilst affecting the fluxional barrier much less. Transposing the substituents (entry **8**) actually results in a 6 kcal mol^{-1} increase in the barrier to reaction compared to X = Y = H, reflecting the nucleophilic nature of the

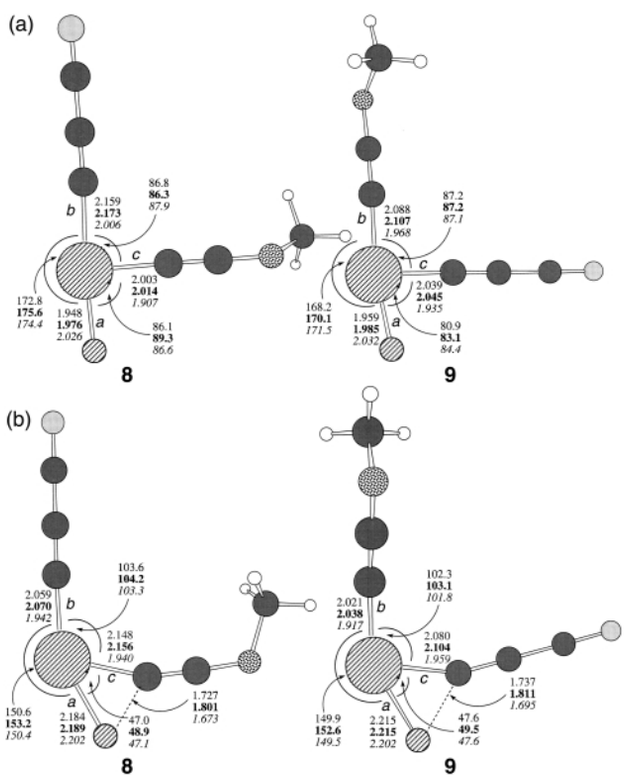

Fig. 2 Distances (Å) and angles (degrees) for (a) the ground states of **8** and **9** and (b) transition states for F–C extrusion. (RHF/3-21G(d), **B3LYP/3-21G(d)**, *MNDOD*).

reaction. The F–R′ extrusion reaction for **8** *vs.* **9** can therefore be regarded as showing a stereoelectronic bias of approximately 11 kcal mol^{-1} in favour of the latter, since formally at least, the difference between the two reactions originates purely from the relative orientations of the iodine lone pairs and the I–F and I–C σ bonds. Typically, for example, stereoelectronic effects at carbon centres such as the anomeric interaction between oxygen lone pairs with C–O σ bonds[38] rarely exceeds about 5 kcal mol^{-1}, which makes this stereoelectronic control at an iodine centre an unusually large effect.

The ground state geometries for **8** and **9** together with the F–R′ extrusion transition states are shown in Fig. 2. Effectively,

Table 3 Energies (activation barriers, kcal mol^{-1}) and first normal mode (cm^{-1}) for the stationary point structures (RHF/3-21G(d)/Hartree, **B3LYP/3-21G(d)/Hartree**, *MNDODL/kcal mol*$^{-1}$)

Entry	F–R′ extrusion	ν_1, ν_2	F_{ax-ax} interconversion	ν_1, ν_2
10,[a] W = I, Z = F, X = SiH_3, Y = H	−7426.9402 (43.1)	636 *i*	−7426.9498 (37.1)	261 *i*
	−7431.7065 (25.7)	**457** *i*	**−7431.7096 (2.38)**	**190** *i*
	157.9 (61.2)	*939 i*	*117.0 (20.3)*	*156 i*
11,[a] W = I, Z = F, X = H, Y = SiH_3	−7426.9456 (39.7)	591 *i*	−7426.9498 (37.0)	261 *i*
	−7431.7102 (23.3)	**426** *i*	**−7431.7096 (23.7)**	**190** *i*
	151.8 (53.0)	*844 i*	*117.0 (18.2)*	*156.i*
12,[b] W = I, Z = F, X = CN, Y = SiH_3	−7518.1600 (43.7)	622 *i*	−7518.1662 (39.8)	260 *i*
	−7523.4468 (25.8)	**448** *i*	**−7523.4478 (25.3)**	**198** *i*
	181.5 (55.9)	*866 i*	*145.4 (19.8)*	*154 i*
13,[b] W = I, Z = F, X = SiH_3, Y = CN	−7518.1677 (35.0)	553 *i*	−7518.1662 (36.0)	260 *i*
	−7523.4522 (19.7)	**399** *i*	**−7523.4478 (22.5)**	**198** *i*
	178.9 (52.6)	*849 i*	*145.4 (19.1)*	*154 i*
14,[c] W = Br, Z = F, X = CN, Y = OCH_3	−3015.0612 (29.2)	633 *i*	−3015.0522 (34.8)	253 *i*
	−3019.4325 (16.2)	**456** *i*	**−3019.4247 (21.1)**	**198** *i*
	166.8 (44.6)	*838 i*	*−131.7 (9.5)*	*121 i*
15,[c] W = Br, Z = F, X = OCH_3, Y = CN	−3015.0829 (11.0)	467 *i*	−3015.0522 (30.3)	253 *i*
	−3019.4484 (2.4)	**253** *i*	**−3019.4247 (17.3)**	**198** *i*
	162.0 (37.0)	*770 i*	*131.7 (6.7)*	*121 i*
16,[d] W = Cl, Z = F, X = CN, Y = OCH_3	−912.1487 (14.2)	612 *i*	−912.1222 (30.8)	243 *i*
	−915.4553 (6.6)	**427** *i*	**−915.4318 (21.4)**	**227** *i*
	166.4 (42.6)	*796 i*	*126.5 (2.7)*	*95 i*
17,[d] W = Cl, Z = F, X = OCH_3, Y = CN	−912.1670 (0.9)	320 *i*	−912.1222 (29.0)	243 *i*
	[e]		**−915.4318**[e]	**227** *i*
	158.9 (33.6)	*722 i*	*126.5 (1.1)*	*95 i*
18,[f] W = I, Z = Cl, X = CN, Y = OCH_3	−7701.2476 (51.4)	660 *i*	−7701.2901 (24.7)	113 *i*
	−7706.8835 (34.4)	**448** *i*	**−7706.9085 (18.7)**	**114** *i*
	161.5 (42.8)	*588 i*	*131.2 (12.4)*	*78 i*
19,[f] W = I, Z = Cl, X = OCH_3, Y = CN	−7701.2739 (30.5)	429 *i*	−7701.2901 (20.3)	113 *i*
	−7706.9041 (17.9)	**287** *i*	**−7706.9085 (15.1)**	**114** *i*
	153.9 (33.1)	*398 i*	*131.2 (0.4)*	*78 i*
20,[g] W = I, Z = CN, X = CN, Y = OCH_3	−7335.5804 (57.5)	879 *i*	−7335.6036 (42.9)	222 *i*
	−7341.0478 (37.0)	**625** *i*	**−7341.0505 (35.4)**	**240** *i*
	229.1 (48.8)	*879 i*	*206.6 (26.3)*	*201 i*
21,[g] W = I, Z = CN, X = OCH_3, Y = CN	−7335.6009 (38.6)	719 *i*	−7335.6036 (37.0)	222 *i*
	−7341.0602 (23.9)	**546***i*	**−7341.0505 (30.0)**	**240** *i*
	224.1 (40.5)	*835 i*	*206.6 (23.0)*	*201 i*

[a] Relative ground state energy **11**–**10**; −0.06, **−0.11**, *−2.09* kcal mol^{-1}; Relative transition state energy **11**–**10**; +3.39, **+2.32**, *+6.16* kcal mol^{-1}. [b] Relative ground state energy **13**–**12**; −3.89, **−2.74**, *−0.71* kcal mol^{-1}; Relative transition state energy **13**–**12**; +4.83, **+3.39**, *+2.58* kcal mol^{-1}. [c] Relative ground state energy **15**–**14**; −4.58, **−3.85**, *−2.81* kcal mol^{-1}. Relative transition state energy **15**–**14**; +13.61, **+9.98,** *+4.77* kcal mol^{-1}. [d] Relative ground state energy **17**–**16**; −1.82, see footnote *e*, *−1.60* kcal mol^{-1}; Relative transition state energy **17**–**16**; +11.48, **e**, *+7.42* kcal mol^{-1}. [e] Ground state structure converges to the products on optimisation. [f] Relative ground state energy **19**–**18**; −4.39, **−3.58**, *−2.02* kcal mol^{-1}; Relative transition state energy **19**–**18**; +16.50, **+12.93**, *+7.59* kcal mol^{-1}. [g] Relative ground state energy **21**–**20**; −5.95, **−5.35**, *−3.32* kcal mol^{-1}; Relative transition state energy **21**–**20**; +12.86, **+7.78**, *+4.99* kcal mol^{-1}.

the length for bond *b* (Fig. 2) is smaller for compound **9** than for compound **8** whilst the length for bond *a* is longer. The length for bond *c* is longer also for compound **9** because of the withdrawing effect of the cyano substituent, making the carbon attached to the iodine more electron deficient. This situation would favour the nucleophilic attack of the fluoride.

The computed barriers for the C–C extrusion were significantly higher than for F–C extrusion, and were much less influenced by the substituents. This is in agreement with the experimental observation that the C–C extrusion is a very minor process.

4. Substituent effects in the monomeric reaction induced by variation in groups W, Z and X

As noted above, an electron donating group X = methoxy can be used to direct F–R′ insertion to the other iodine–alkynyl or aryl group. The methoxy substituent however can create significant synthetic problems during the preparation of the diaryl iodonium salts. We decided to try an alternative electropositive group such as SiH_3 as a model group to see if that might be a more effective directing group. The results (Table 3) indicate that SiH_3 in fact reveals a preference for equatorial F–R′ insertion (entries **11**–**13**), and would not achieve the desired effect. We also explored other variations of the basic substituents such as the central group W and the nucleophilic group Z (Table 1 and Table 3). The substitution of W = I by W = Br, Cl led to substantial decreases of the activation barriers for extrusion, but in the case of Cl at least is likely to lead to such high energies for the starting R_2Cl^+ chloronium ions as to preclude facile synthesis.[29] An unexpected result was obtained for the bromine derivatives (entries **14** and **15**). Here the computed barriers for the R/R′ interconversion of the Z = F *via* a monomeric unit were larger than for the F–R′ extrusion. This aspect is discussed further in the section on dimers below. Finally, we note that replacing Z = F by Z = Cl as a nucleophile (entry **18** and **19**) results in very similar specificity to F, and almost identical barriers to extrusion. Likewise, Z = CN (entries **20** and **21**) shows characteristics very similar to Z = F.

5. NBO analysis of the reaction specificities[39]

We carried out a natural bond orbital (NBO) analysis of the ground and transition states for some of the species in order to understand the factors that control their relative stabilities. The most significant difference found between the isomers **8** and **9** at the ground state corresponds to the interaction $n_\pi(F)$ to σ^* ($I–C_x$) which is 142.4 kcal mol^{-1} for the isomer **8** and 112.9 kcal mol^{-1} for the isomer **9** at the RHF/3-21G(d) level (Table 4). This is in agreement with a shorter bond length for the F–I bond for the isomer **8**. This is due to the difference in energy between both orbitals (0.78 Hartree for **8** and 0.82 Hartree for

Table 4 Energies for the interaction between a donor orbital (i) and an acceptor orbital (j) (RHF/3-21G(d)/kcal mol^{-1}, **B3LYP/3-21G(d)/kcal mol^{-1}**)

	Interaction $n_\pi(F)$ to $\sigma^*(W–C_x)$			
	GS		TS (F–C) extrusion	
	E	$E_j - E_i$	*E*	$E_j - E_i$
8	142.4/**105.5**	0.78/**0.43**	51.6/**38.7**	0.86/**0.45**
9	112.9/**84.5**	0.82/**0.46**	43.8/**33.7**	0.86/**0.45**
14	182.5/**135.6**	0.64/**0.33**	54.7/**43.6**	0.69/**0.37**
15	128.9/**95.3**	0.70/**0.37**	66.4/**47.8**	0.78/**0.41**
16	145.7/**124.0**	0.67/**0.27**	58.6/**42.0**	0.76/**0.38**
17	85.2/[a]	0.76/[a]	52.1/[a]	0.84/[a]
	Interaction $n_\pi(F)$ to $\sigma^*(W–C_y)$			
	GS		TS (F–C extrusion)	
	E	$E_j - E_i$	*E*	$E_j - E_I$
8	24.6/**15.1**	0.83/**0.46**	50.6/**35.2**	0.59/**0.29**
9	34.4/**22.2**	0.80/**0.43**	28.5/**20.8**	0.64/**0.31**
14	11.4/**6.1**	0.80/**0.44**	20.5/**16.1**	0.73/**0.33**
15	16.8/**9.8**	0.77/**0.40**	8.6/**5.8**	0.68/**0.32**
16	7.4/**2.4**	0.86/**0.46**	13.8/**8.3**	0.71/**0.34**
17	6.5/[a]	0.82/[a]	6.1/[a]	0.75/[a]
	Interaction $n_\pi(F)$ to $\pi^*(C_y{\equiv}C)$ except $n_\pi(F)$ to $\sigma^*(C_y{\equiv}C)$ for **6** (B3LYP), **7** (B3LYP) and transition state for **15** (RHF)			
	GS		TS (F–C extrusion)	
	E	$E_j - E_i$	*E*	$E_j - E_I$
8	[b]		52.8/**34.9**	0.87/**0.48**
9	[b]		90.2/**51.7**	0.77/**0.43**
14	[b]		43.4/**29.7**	0.94/**0.50**
15	[b]		37.0/**23.6**	0.70/**0.35**
			14.3/**11.0**	0.80/**0.44**
16	[b]		28.5/**20.1**	0.76/**0.40**
			14.4/**9.2**	0.80/**0.47**
17	11.47/[a]	0.72/[a]	52.1/[a]	0.84/[a]
			6.6/[a]	1.69/[a]

[a] Ground state structure converges to the products on optimisation. [b] This interaction does not exist or is insignificant.

9) and explains the greater stability of compound **8**. This difference in the interaction $n_\pi(F)$ to σ^* ($I–C_x$) is more intense for the bromine derivatives (182.5 kcal mol^{-1} for the isomer **14** and 128.9 kcal mol^{-1} for the isomer **15**) and even more for the chlorine derivatives (145.7 kcal mol^{-1} for the isomer **16** and 85.2 kcal mol^{-1} for the isomer **17**).

The $n_\pi(F)$ to σ^* ($I–C_x$) interaction appears much less relevant for the stabilisation of the transition states, due presumably to less favourable orbital overlaps at this geometry. The interaction $n_\pi(F)$ to σ^* ($I–C_y$) is reduced to 50.6 kcal mol^{-1} for **8** and 28.5 kcal mol^{-1} for **9**. Instead, another interaction shows a large difference in the opposite sense between the two systems, *i.e.* that between $n_\pi(F)$ and $\sigma^*(C_y{\equiv}C)$ which is 52.8 kcal mol^{-1} for **8** and 90.2 kcal mol^{-1} for **9**. The key to explaining the greater stability of the transition state **9** is the combination of a destabilising effect of the fluorine towards the $I–C_y$ bond plus a stabilising effect of the fluorine towards the $C_y{\equiv}C$ bond. It is remarkable that the magnitude of the interaction of both effects ($n_\pi(F)$ to $\sigma^*(I\text{-}C_y)$ and $n_\pi(F)$ to $\pi^*(C_y{\equiv}C)$) is very similar for **8**, while the interaction $n_\pi(F)$ to $\pi^*(C_y{\equiv}C)$ is much bigger than the interaction $n_\pi(F)$ to $\sigma^*(I–C_y)$ for **9**. This is consistent with a longer length for the F–I bond for **9**, indicating a much more product-like geometry for **9** than for **8**. This effect is more noticeable for the bromo and the chloro reagents where the interaction $n_\pi(F)$ to $\sigma^*(I–C_y)$ is very weak for **15** and **17** (8.8 and 6.1 kcal mol^{-1}). The bigger stabilisation of their transition states is due to the strong interaction $n_\pi(F)$ to $\pi^*(C_y{\equiv}C)$ for the isomer **15** (the total value is 51.3 kcal mol^{-1}) and $n_\pi(F)$ to $\sigma^*(C_y{\equiv}C)$ for the isomer **17** (the total value is 58.7 kcal mol^{-1}).

6. Effect of dimer formation on the reaction energetics

Having established the basic characteristics of the potential energy surface for the reaction monomers, we next investigated the effect of dimer formation for the model systems **22**–**26** shown in Scheme 4. The dimerisation energies decrease slightly

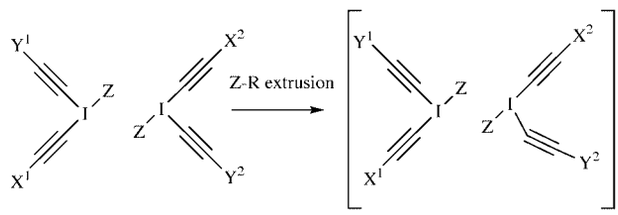

Scheme 4

along the series Z = F to Br (Table 5), but are substantial in all cases. For Z = F, the *ab initio* geometries are calculated to be significantly asymmetric (I–F 2.0, 2.5–2.7 Å), whereas the MNDO-d geometry is symmetric (Fig. 3). At the *ab initio* level at least, this implies that the distinction between the R and R′ groups is also preserved in the dimeric species. This asymmetry is what might have been anticipated from consideration purely of the van der Waals radius of iodine. Thus the asymmetric distortion results in an I–I distance (4.0–4.2 Å) similar to that found in the crystal structure for Z = Cl, which exhibits only

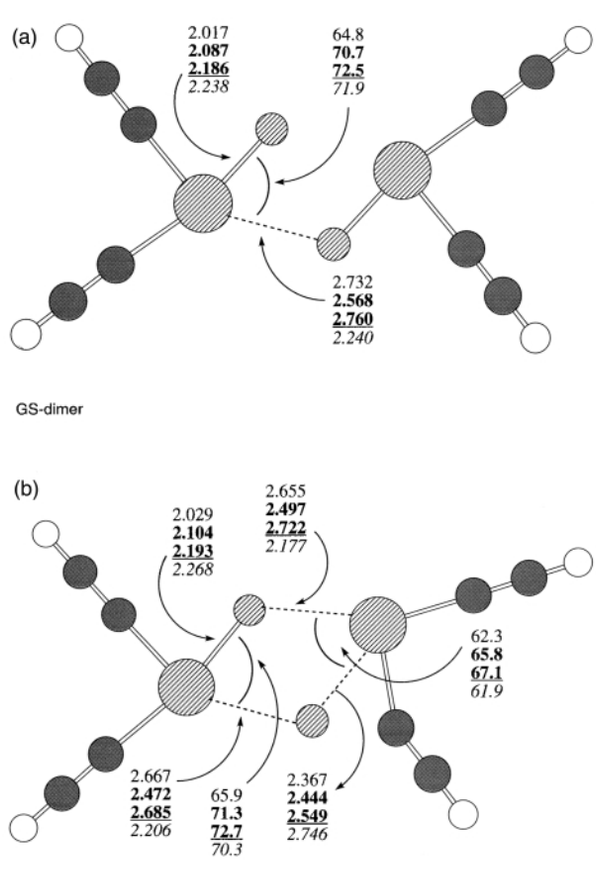

Fig. 3 Geometry (distances in Å and angles in degrees) for (a) the ground states of **22** and (b) the transition states of **22** (RHF/3-21G(d), **B3LYP/3-21G(d)**, **B3LYP/DZVP**, *MNDOD*).

Table 5 Energies (dimerisation/activation) and first normal mode (cm^{-1}) for stationary point structures (RHF/3-21G(d)/Hartree. RHF/MIDI!/Hartree, **B3LYP/3-21G(d)/Hartree**, **B3LYP/MIDI!/Hartree**, ***B3LYP/DZVP/Hartree***, *MNDOD/kcal mol*$^{-1}$)

Entry	GS	TS F–R′ extrusion	ν_1	TS F_{ax-ax} interconversion [a]	ν_1
22, $X^1 = Y^1 = H$, $X^2 = Y^2 = H$	−14276.7220 (18.2)[b]	−14276.6557 (41.6)[c]	583 *i*	−14276.7010 (13.2)[d]	223 *i*
	−14275.5576 (14.1)	−14275.4873 (44.1)	652 *i*		
	−14284.9882 (24.3)	**−14284.9473 (25.7)**	**418** *i*	**−14284.9837 (2.8)**	**99** *i*
	−14283.8232 (19.9)	**−14283.7808 (26.6)**	**489** *i*		
	−14346.2180 (13.9)	***−14346.1794 (24.2)***	***413*** *i*	***−14346.2132 (3.0)***	***115*** *i*
	192.8 (21.2)	*247.7 (54.8)*	*794 i*	0.0	
23, X^1 = CN, $Y^1 = OCH_3$,	−14685.6669 (18.1)	−14685.5851 (51.3)	633 *i*	−14685.6377 (18.3)	216 *i*
X^2 = CN, $Y^2 = OCH_3$	**−14696.2596 (24.4)**	**−14696.2081 (32.2)**	**454** *i*	**−14696.2498 (6.1)**	**61** *i*, **2** *i*
	163.4 (22.4)	*217.2 (53.8)*	*809 i*	0.0	
24, X^1 = CN, $Y^1 = OCH_3$,	−14685.6597 (18.7)	−14685.6088 (31.9)	486 *i*	−14685.6381 (13.6)	214 *i*
$X^2 = OCH_3$, Y^2 = CN	**−14696.2547 (25.0)**	**−14696.2255 (18.3)**	**344** *i*	**−14696.2506 (2.6)**	**92** *i*
	164.3 (22.3)	*212.7 (48.4)*	*740 i*	0.0	
25, $X^1 = OCH_3$, Y^1 = CN,	−14685.6529 (19.7)	−14685.6028 (31.5)	481 *i*	−14685.6377 (9.6)	216 *i*
$X^2 = OCH_3$, Y^2 = CN	**−14696.2506 (26.1)**	**−14696.2221 (17.9)**	**328** *i*	**−14696.2498 (0.5)**	**61** *i*, **2** *i*
	163.4 (26.0)	*211.8 (48.4)*	*744 i*	0.0	
26, $X^1 = OCH_3$, Y^1 = CN,	−14685.6597 (18.7)	−14685.5791 (50.6)	621 *i*	−14685.6381 (13.6)	214 *i*
X^2 = CN, $Y^2 = OCH_3$	**−14696.2547 (25.0)**	**−14696.2137 (25.8)**	**430** *i*	**−14696.2506 (2.6)**	**92** *i*
	164.3 (23.3)	*216.1 (51.8)*	*812 i*	0.0	

[a] MNDO-d predicts a symmetrical dimer. [b] Corresponding values for Z = Cl; −14993.7433 (16.1) Z = Br; −19199.4820 (17.1). [c] Corresponding values for Z = Cl, −14993.6685 (46.9). [d] Corresponding value for Z = Cl; 0.0.

very slight asymmetry. The predicted geometry for the Z = Cl dimer is also symmetric.

When the dimeric structure is considered, an entirely new mechanism involving a symmetrically bridged structure becomes available for R/R′ interconversion, as an alternative to that proposed by Grushin.[5] This symmetric bridge is characterised as a transition state at the *ab initio* level, with a barrier ranging from 15 kcal mol^{-1} (RHF-3-21G*) to 3 kcal mol^{-1} (B3LYP/DZVP) (Table 5). The process can be envisaged as a form of dyotropic reaction involving mutual F exchange between monomers, or more pictorially as a form of molecular metronome. We also reiterate the observation for other systems that sterically large R groups can inhibit dimer formation, and in these instances R/R′ interconversion may indeed have to proceed through the monomer mechanism, or involve a substantially higher barrier for the metronome process. Specifically for the RR′Br–F system noted earlier, this might result in a R–F extrusion reaction where the specificity for R or R′ would be determined by the relative stability of the RR′Br–F reagents rather than being controlled by the stereoelectronic effects in the extrusion transition states.

Transition states for the F–R′ extrusion reaction starting from dimer were readily located, using as starting geometries those of the monomeric stationary points (Fig. 3). The influence of electron withdrawing or donating groups within R were virtually identical to the monomer values, and furthermore additive (entries **23**–**26**, Table 5). Thus F–R extrusion is enhanced by an electron withdrawing group on the reacting R centre and inhibited by an electron donating group. The transition state was stabilised by dimer formation by a very similar value calculated for the stabilisation of ground state itself. This implies that the barrier to reaction as a dimer is actually quite similar to that for the momomer itself. Finally, we noted that an electron withdrawing group present in the pseudo axial position of the non-reacting component of the dimer stabilised the transition state by a similar amount to that found for the presence of such a substituent in the monomer ground state.

Conclusions

The trivalent RR′I–F iodine(III) system at the centre of this set of reactions induces some unusual and unique features not normally encountered in carbon based chemistry. The d-orbital participation at the halogen centre results in the "T" geometry for these species, and very specific preferences for occupation of the three different ligands, with the fluorine favouring one axial position, and carbon ligands bearing electron withdrawing groups favouring the other axial position over groups bearing electron donating groups. Two types of reaction at this centre can occur, one involving interconversion of the ligands *via* three different transition states, and the other involving the formation of iodine(I) *via* extrusion and concomitant F–R or R–R′ bond formation. The balance between these reaction pathways, and the F–R reaction in particular is very sensitive to substituent effects. These stabilise the F–R transition state in the opposite sense to that found for the ground state, and can therefore be regarded as novel examples of stereoelectronic control at a non-carbon centre. We predict that the basic reaction might be able to tolerate other variations, such as replacement of Z = F by Cl or CN to allow nucleophilic chlorination or cyanation, or replacement of the central atom (W = I) by *e.g.* bromine.

We note on the basis of homologous crystal structures that R_2I–F is expected to form a stable dimer, which our calculations predict will actually have a novel unsymmetric bridge. The subsequent reactivity of this dimer closely resembles that of the monomeric units. One novel feature of the dimer formation is that it provides an alternative, hitherto unconsidered, low energy pathway for R/R′ interconversion, which strongly indicates that the specificity of these reactions is purely transition state controlled. Further explorations of trimer and tetrameric reaction paths will be reported in a future paper.

Acknowledgements

We thank the EPSRC for financial support.

References

1 A. Varvoglis, *Chem. Soc. Rev.*, 1981, **10**, 377; A. Varvoglis, *Synthesis*, 1984, 709; R. M. Moriarty and O. Prakash, *Acc. Chem. Res.*, 1986, **19**, 244; P. J. Stang and V. V. Zhdankin, *Chem. Rev.*, 1996, **96**, 1123; A. Varvoglis, *Hypervalent Iodine in Organic Synthesis*, Academic Press, London, 1997.

2 A. Shah, V. W. Pike and D. A. Widdowson, *J. Chem. Soc.*, *Perkin Trans. 1*, 1997, 2463; V. W. Pike, F. Butt, A. Shah and D. A. Widdowson, *J. Chem. Soc.*, *Perkin Trans 1*, 1999, 245.

3 M. S. Ermolenko, V. A. Budylin and A. N. Kost, *J. Heterocyl. Chem.* (*Engl. Trans.*), 1978, 752; M. van der Puy, *J. Fluorine Chem.*, 1982, **21**, 385.
4 V. W. Pike and F. I. Aigbirhio, *J. Chem. Soc.*, *Chem. Commun.*, 1995, 2215; A. Shah, V. W. Pike and D. A. Widdowson, *J. Chem. Soc.*, *Perkin Trans. 1*, 1998, 2043; A. Shah, D. A. Widdowson and V. W. Pike, *J. Labelled Compd. Radiopharm.*, 1997, **39**, 65.
5 V. V. Grushin, *Acc. Chem. Res.*, 1992, **25**, 529; V. V. Grushin, I. I. Demkina and T. P. Tolstaya, *J. Chem. Soc.*, *Perkin Trans 2*, 1992, 505 and refs. therein.
6 M. Guillaume, A. Luxen, B. Nebeling, M. Argentini, J. C. Clark and V. W. Pike, *Appl. Radiat. Isot.*, 1991, **42**, 749.
7 M. J. Phelps, J. Mazziotta and H. Schelbert, *Positron Emission Tomography and Autoradiography: Principles and Applications for the Brain and Heart*, Raven Press, New York, 1986.
8 A. Luxen, M. Guillaume, W. P. Melega, V. W. Pike, O. Solin and R. Wagner, *Nucl. Med. Biol.*, 1992, **19**, 149; E. S. Garnett, G. Firnau and C. Nahmias, *Nature*, 1983, **305**, 137.
9 K. M. Lancer and G. H. Wiegand, *J. Org. Chem.*, 1976, **41**, 3360; G. A. Olah, T. Sakakibara and G. Asensio, *J. Org. Chem.*, 1978, **43**, 463.
10 A. I. Boldyrev, V. V. Zhdankin, J. Simons and P. J. Stang, *J. Am. Chem. Soc.*, 1992, **114**, 10569; P. Schwerdtfeger, *J. Phys. Chem.*, 1996, **100**, 2968.
11 B. M. Bode and M. S. Gordon, *J. Mol. Graphics Mod.,* 1998, 133.
12 M. W. Schmidt, K. K. Baldridge, J. A. Boatz, S. T. Elbert, M. S. Gordon, J. H. Jensen, S. Koseki, N. Matsunaga, K. A. Nguyen, S. Su, T. L. Windus, M. Dupuis and J. A. Montgomery, *J. Comput. Chem.*, 1993, **14**, 1347.
13 GAUSSIAN98 (Revision A.1), M. J. Frisch, G. W. Trucks, H. B. Schlegel, G. E. Scuseria, M. A. Robb, J. R. Cheeseman, V. G. Zakrzewski, J. A. Montgomery, R. E. Stratmann, J. C. Burant, S. Dapprich, J. M. Millam, A. D. Daniels, K. N. Kudin, M. C. Strain, O. Farkas, J. Tomasi, V. Barone, M. Cossi, R. Cammi, B. Mennucci, C. Pomelli, C. Adamo, S. Clifford, J. Ochterski, G. A. Petersson, P. Y. Ayala, Q. Cui, K. Morokuma, D. K. Malick, A. D. Rabuck, K. Raghavachari, J. B. Foresman, J. Cioslowski, J. V. Ortiz, B. B. Stefanov, G. Liu, A. Liashenko, P. Piskorz, I. Komaromi, R. Gomperts, R. L. Martin, D. J. Fox, T. Keith, M. A. Al-Laham, C. Y. Peng, A. Nanayakkara, C. Gonzalez, M. Challacombe, P. M. W. Gill, B. G. Johnson, W. Chen, M. W. Wong, J. L. Andres, M. Head-Gordon, E. S. Replogle and J. A. Pople, Gaussian, Inc., Pittsburgh, PA, 1998.
14 MOPAC2000, J. J. P. Stewart, Fujitsu Limited, Tokyo, Japan, 1999.
15 F. H. Allen and O. Kennard, *Chem. Des. Automat. News*, 1993, **8**, 1, 31.
16 P. J. Stang, A. M. Arif and C. M. Crittell, *Angew. Chem.*, *Int. Ed. Engl.*, 1990, **29**, 287.
17 A. P. Bozopoulos, C. A. Kavounis, G. S. Stergioudis and P. J. Rentzeperis, *Z. Kristallogr.*, 1989, **187**, 97.
18 N. W. Alcock and R. M. Countryman, *J. Chem. Soc.*, *Dalton Trans.*, 1977, 217; 1987, 193.
19 Active models demonstrating these features for all these structures are included in the on-line supplementary data for this article.
20 V. V. Bardin, T. Fiefhaus, H. J. Frohn, A. Klose, R. Nielinger, A. Priwitzer and T. Schroer, *J. Fluorine Chem.*, 1995, **71**, 183.
21 J. V. Carey, P. A. Chaloner, P. B. Hitchcock, T. Neugebauer and K. R. Seddon, *J. Chem. Res.*, 1996, **348**, 358.
22 A. K. Mishra, M. M. Olmstead, J. J. Ellison and P. P. Power, *Inorg. Chem.*, 1995, **34**, 3210.
23 P. J. Stang, B. W. Surber, Z.-C. Chen, K. A. Roberts and A. G. Anderson, *J. Am. Chem. Soc.*, 1987, **109**, 228.
24 V. V. Zhdankin, S. A. Erickson and K. J. Hansen, *J. Am. Chem. Soc.*, 1997, **119**, 4775.
25 W. B. Wright and E. A. Meyers, *Cryst. Struct. Commun.*, 1972, **1**, 95.
26 N. W. Alcock, R. M. Countryman, S. Esperas and J. F. Sawyer, *J. Chem. Soc.*, *Dalton Trans.*, 1979, 854.
27 M. Ochiai, Y. Masaki and M. Shiro, *J. Org. Chem.*, 1991, **56**, 5511.
28 A. N. Nesmeyanov, T. L. Khotsyanova, V. V. Saatsazov, T. P. Tolstaya and L. S. Isaeva, *Dokl. Akad. Nauk SSSR*, 1974, **218**, 140.
29 T. Mori, R. Rathore, S. V. Lindeman and J. K. Kochi, *J. Chem. Soc.*, *Chem. Commun.*, 1998, 927. See also R. S. Brown, R. W. Nagorski, A. J. Bennet, R. E. D. McClung, G. H. M. Aarts, M. Klobukowski, R. McDonald and B. D. Santarsiero, *J. Am. Chem. Soc.*, 1994, **116**, 2448 for a similar structure for a RR′Br–OTf derivative.
30 T. Kreuter and B. Neumuller, *Z. Anorg. Allg. Chem.*, 1995, **621**, 597.
31 J. T. Leman and A. R. Barron, *Organometallics*, 1989, **8**, 2214.
32 A. H. Cowley, H. S. Isom and A. Decken, *Organometallics*, 1995, **14**, 2589.
33 K. Henrick, M. McPartlin, R. W. Matthews, G. B. Deacon and R. J. Phillips, *J. Organomet. Chem.*, 1980, **193**, 13.
34 R. Koster, W. Schussler and R. Boese, *Chem. Ber.*, 1990, **123**, 1945.
35 N. Godbout, D. R. Salahub, J. Andzelm and E. Wimmer, *Can. J. Chem.*, 1992, **70**, 560.
36 A. J. Sadlej, *Theor. Chim. Acta*, 1992, **81**, 339.
37 For some representative examples of this limitation see: F. Jensen and K. N. Houk, *J. Am. Chem. Soc.*, 1987, **109**, 3139; W. L. Jorgensen, D. Lim and J. F. Blake, *J. Am. Chem. Soc.*, 1993, **115**, 2936; K. N. Houk, L. Gonzalez and Y. Li, *Acc. Chem. Res.*, 1995, **28**, 81; S. Ham and D. M. Birney, *Tetrahedron Lett.*, 1997, **38**, 5925.
38 P. Deslongchamps, Y. L. Dory and A. G. Li, *Can. J. Chem.*, 1994, **72**, 2021.
39 P. v. R. Schleyer, M. Kaupp, F. Hampel, M. Bremer and K. Mislow, *J. Am. Chem. Soc.*, 1992, **114**, 6791; T. Yamamoto and S. Tomodo, *Chem. Lett.*, 1997, 1069.

Paper 9/06212B